



Effects of acetonitrile on electrodeposition of Ni from a hydrophobic ionic liquid

Yan-Li Zhu, Yasushi Katayama^{*,1}, Takashi Miura

Department of Applied Chemistry, Faculty of Science and Technology, Keio University, Hiyoshi, 3-14-1, Kohoku-ku, Yokohama, Kanagawa 223-8522, Japan

ARTICLE INFO

Article history:

Received 11 May 2010

Received in revised form 30 July 2010

Accepted 30 July 2010

Available online 18 August 2010

Keywords:

Electrodeposition

Nickel

Acetonitrile

Ionic liquid

1-butyl-1-methylpyrrolidinium

Bis(trifluoromethylsulfonyl)amide

ABSTRACT

The effects of addition of acetonitrile (ACN) on electrodeposition of nickel were investigated in a hydrophobic room-temperature ionic liquid, 1-butyl-1-methylpyrrolidinium bis(trifluoromethylsulfonyl)amide (BMPTFSA) containing Ni(TFSA)₂. Addition of ACN resulted in the change of the color of the ionic liquid. The UV–vis and FT-IR spectra of the electrolyte showed the coordination environment of Ni(II) changed gradually from [Ni(TFSA)₃]⁻ to [Ni(ACN)₆]²⁺ with an increase in the concentration of ACN. The diffusion coefficient of Ni(II) in BMPTFSA was increased and the reduction potential of Ni(II) shifted to the more positive side in the presence of ACN. The nucleation/growth process of Ni was not affected by the change in the coordination environment of Ni(II) from the chronoamperometric results although the more nuclei formed on the electrode surface. SEM showed smoother deposit was obtained in Ni(TFSA)₂/BMPTFSA with ACN.

© 2010 Elsevier Ltd. All rights reserved.

1. Introduction

Much interest in the electrodeposition of nickel and nickel-based alloys is due to their variety of commercial applications, such as decoration, corrosion and heat resistance, magnetic recording devices, etc [1–3]. Technological developments in recent years like microelectromechanical systems require Ni or its alloy, which exhibit optimal performance with a smooth surface morphology since the morphology is one of the important characteristics and influences the material properties [4–6].

Nickel or its alloys are generally electrodeposited from chloride, sulfate, sulfamate and Watts-type electrolytes [4,7]. However, the electrochemical deposition from these aqueous systems often involves the evolution of hydrogen, which deteriorates the quality of the deposits. Room-temperature ionic liquids composed of bis(trifluoromethylsulfonyl)amide (TFSA⁻) have attracted much attention in the electrochemical field because of its hydrophobicity. In addition, they have high thermal stability and negligible vapor pressure [8]. These merits make the ionic liquids be favorable to the practical applications.

It is well-known that organic additives added at small concentrations to electroplating baths have various effects on the morphology and structure of the electrodeposited Ni or its alloys

and then change their related properties. The additives have been studied extensively in aqueous solutions [6,7,9–17]. Some of them may reduce pitting and internal stress, leading to improvement of the property of the deposit. The activity of an organic additive mainly depends on the presence of certain types of unsaturations among atoms of carbon, nitrogen, and oxygen (or certain sulfur-containing radicals) [18]. On the other hand, a few studies have been reported in room-temperature ionic liquids. Abbott and his co-workers have reported the effects of ethylenediamine (en) and acetylacetonate (acac) on the Ni electrodeposition in either a urea or ethylene glycol/choline chloride based ionic liquid [19]. The morphologies of Ni deposits can be changed after addition these two additives. Both the additives suppressed the under potential deposition of Ni on a platinum electrode and led to give finer-grained deposits. Wang and co-workers also found the similar behaviors for Co electrodeposition after adding 2-butyne-1,4-diol into 1-ethyl-3-methylimidazolium (EMI) and ethylene glycol containing cobalt chloride [20]. 2-Butyne-1,4-diol could also suppress the under potential deposition of Co and smaller grain size of Co deposits could be obtained in the presence of the additive. Wallace and co-workers used pyrrol as an additive to induce deposition of titanium species from EMIMTFSA containing TiCl₄ [21]. However, there are still a few reports about the effects of additives on the electrodeposition of metals from ionic liquids up to now.

We have already reported the electrochemical behavior of Ni(II)/Ni in BMPTFSA (BMP⁺: 1-butyl-1-methylpyrrolidinium) containing Ni(TFSA)₂ as a Ni source, and the XRD showed that the metallic Ni could be obtained from this ionic liquid successfully [22]. In the present study, the effects of the organic additive of ace-

* Corresponding author. Tel.: +81 45 566 1561; fax: +81 45 566 1561.

E-mail address: katayama@applic.keio.ac.jp (Y. Katayama).

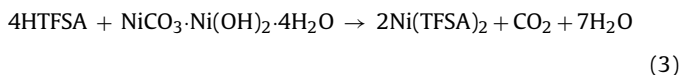
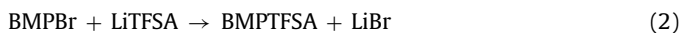
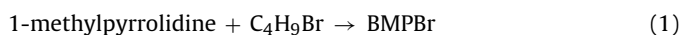
¹ ISE Member.

tonitrile (ACN) on the electrodeposition of Ni were examined in this ionic liquid.

2. Experimental

All the electrochemical experiments and handling of hygroscopic reagents were performed in an argon-filled glove box with a continuous gas purification apparatus (Miwa Seisakujo Co. Ltd., DB0-1K-SH). The concentrations of both H₂O and O₂ in the gas were kept under 1 ppm.

BMPTFSA and Ni(TFSA)₂ were prepared by the following reactions:



The details about the preparation procedures can be found elsewhere [22]. The water content in BMPTFSA was below 10 ppm, which was determined by Karl Fischer titration (Metrohm, 831 KF Coulometer). Acetonitrile (ACN, Wako, >99.0%, anhydrous) was used as supplied.

Electrochemical measurements and electrodeposition experiments were carried out using a standard three-electrode cell with the aid of a potentiostat/galvanostat (Hokuto Denko, HABF-501). For electrochemical measurements, a platinum disk electrode (7.85 × 10⁻³ cm²) was employed as a working electrode after mirror polishing by 0.05 μm alumina (Baikowski), electrolytic degreasing in an alkaline solution for 1 min, washing with 10 vol% H₂SO₄ and distilled water, and dried in the air. Platinum wire was used as the auxiliary electrode. Silver wire immersed in BMPTFSA containing 0.1 M (mol dm⁻³) AgCF₃SO₃ (Aldrich, >99.0%) was used as a reference electrode. The AgCF₃SO₃/BMPTFSA solution was separated from main electrolyte by porous Vycor glass. For the electrodeposition, a copper disk electrode (7.06 × 10⁻² cm²) was used as a substrate. The pretreatment was the same as the platinum disk. Ni (Nilaco) wire was employed as an auxiliary electrode. The reference electrode was as the same as described above.

The absorption spectra of BMPTFSA containing Ni(TFSA)₂ with and without the additive were measured by UV–vis spectrometer (JASCO, V-530) and Fourier transform infrared spectrophotometer (FT-IR, SHIMADZU, Prestige-21). UV–vis spectra were obtained using an air-tight quartz cell with a light path length of 0.1 cm. The FT-IR spectra of the ionic liquids were measured using an attenuated total reflectance attachment (ATR, ZnSe prism) with an optical resolution of 4 cm⁻¹. The electrodeposits washed with acetone (Wako, >99.8%) and dried in the air were characterized by a scanning electron microscopy (SEM, KEYENCE VE-9800) and energy-dispersive X-ray analysis (EDX, EDAX Phoenix).

3. Results and discussion

In our previous study, the UV–vis spectra indicated the Ni(II) in Ni(TFSA)₂/BMPTFSA was octahedrally coordinated by TFSA⁻ [22]. [Ni(TFSA)₃]⁻ was considered to be formed in this ionic liquid, in which the TFSA⁻ acts as a bidentate ligand [23]. The diffusion coefficient of this Ni species was estimated to be 9.3 × 10⁻⁸ cm² s⁻¹ by chronoamperometry, indicating its mobility is rather low [22]. The reason for this is probably due to the formation of the bulky complexes [24]. In order to change the dissolved Ni(II) species, ACN, which has a larger donor number than TFSA⁻ [24], was added to the electrolyte. It is expected that the coordination environment of

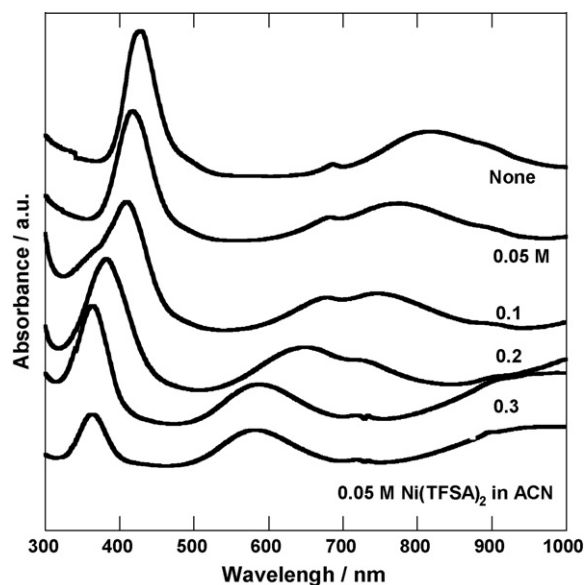


Fig. 1. UV–vis spectra of 0.05 M Ni(TFSA)₂/BMPTFSA with various concentrations of ACN. The spectrum of 0.05 M Ni(TFSA)₂/ACN is also shown.

Ni(II) in BMPTFSA can be changed by ACN, leading to the changes in the electrodeposition process and the morphology of the deposits.

3.1. Solvation structure of Ni(II) in BMPTFSA with ACN

The color of 0.05 M Ni(TFSA)₂/BMPTFSA changed from yellow to blue gradually with an increase in the concentration of ACN. Fig. 1 shows the UV–vis spectra of 0.05 M Ni(TFSA)₂/BMPTFSA with various concentrations of ACN at room-temperature. Two absorption bands around 430 (³T_{1g}(³P) ← ³A_{2g}(³F)) and 815 nm (³T_{1g}(³F) ← ³A_{2g}(³F)) can be assigned to the octahedrally coordinated complexes of Ni²⁺ and TFSA⁻. Both maxima of these bands shifted to the shorter wavelengths with an increase in the concentration of ACN. When 0.3 M ACN was added into the ionic liquid, the molar ratio of ACN to Ni (II) was 6. The absorption bands at around 360 and 588 nm are consistent with those observed in 0.05 M Ni(TFSA)₂/ACN. Thus, this absorption spectrum indicates the formation of the octahedrally coordinated species of [Ni(ACN)₆]²⁺ [25,26]. The change in the coordination environment of Ni(II) can be attributed to the difference in the donor property of the ligands. Since the donor number of ACN (about 14) is larger than that of TFSA⁻ (about 7), [Ni(ACN)₆]²⁺ is expected to be more stable than [Ni(TFSA)₃]⁻ [24]. The absorbance for [Ni(TFSA)₃]⁻ decreased and that for [Ni(ACN)₆]²⁺ increased with an increase in the ACN concentration, indicating TFSA⁻ coordinating Ni²⁺ is replaced with ACN.

Fig. 2 shows FT-IR spectra of BMPTFSA containing various concentrations of Ni(TFSA)₂. It has been known that there are two conformational states in the structure of TFSA⁻: a cisoid form of C₁ symmetry and a transoid form of C₂ symmetry with respect to the S–N–S plane [27]. The intense bands appearing at 1330 and 1348 nm are ascribed to the S–O stretching vibration of C₁-ν_a(SO₂) and C₂-ν_a(SO₂), respectively [28]. As shown in Fig. 2, the absorbance of C₂-ν_a(SO₂) was decreased and C₁-ν_a(SO₂) increased with increasing the concentration of Ni(II) probably due to the TFSA⁻ bound to the Ni²⁺ [23]. Thus, it is possible to estimate the concentration of [Ni(TFSA)₃]⁻ from the ratio of the absorbances of C₁-ν_a(SO₂) and C₂-ν_a(SO₂).

The FT-IR spectra of 0.3 M Ni(TFSA)₂/BMPTFSA with various concentrations of ACN is shown in Fig. 3. The absorbance of stretching of C₂-ν_a(SO₂) became stronger and that of C₁-ν_a(SO₂) became weaker

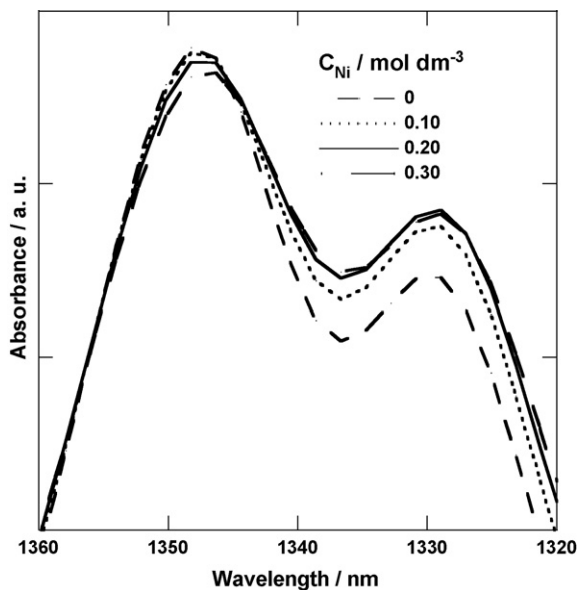


Fig. 2. FT-IR spectra of BMPTFSA with various concentrations of Ni(TFSA)₂.

with an increase in the amount of ACN in the ionic liquid, indicating TFSA⁻ coordinated to Ni²⁺ were replaced with ACN. Moreover, the FT-IR spectra of 0.3 M Ni(TFSA)₂/BMPTFSA with 1.8 M ACN was identical to that for neat BMPTFSA, as shown in Fig. 2. The same spectra of these two electrolytes indicate all of the TFSA⁻ coordinated to Ni(II) species was replaced by ACN and a new kind of Ni(II) species, [Ni(ACN)₆]²⁺ was formed, as anticipated from the UV-vis spectra.

3.2. Cyclic voltammetry

Fig. 4 shows the cyclic voltammograms of a Pt electrode in 0.05 M Ni(TFSA)₂/BMPTFSA with various concentrations of ACN at 25 °C. The potential of cathodic reduction of Ni(II) shifted to the more positive side in the presence of ACN due to the change in the coordination environment of the Ni(II)

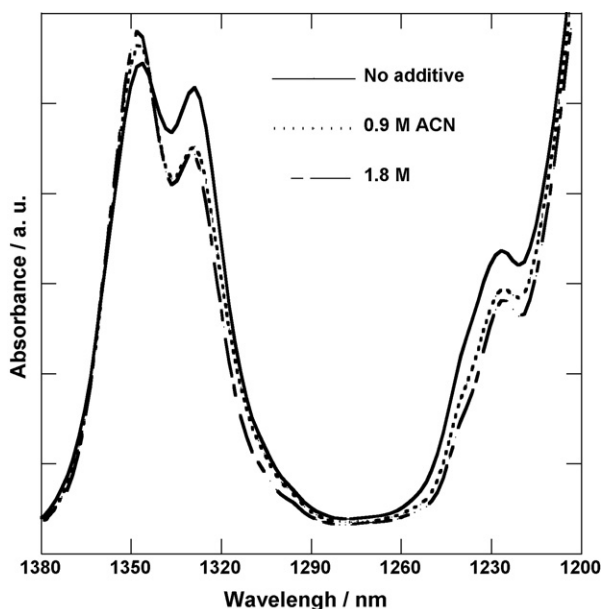


Fig. 3. FT-IR spectra of 0.3 M Ni(TFSA)₂/BMPTFSA with various concentrations of ACN.

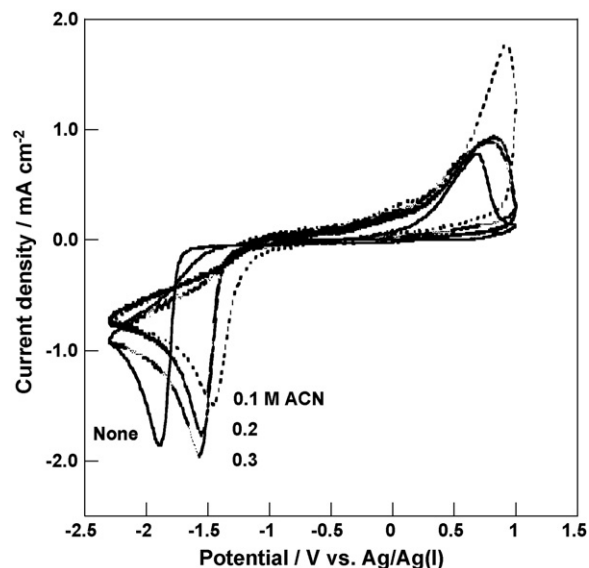


Fig. 4. Cyclic voltammograms of a Pt electrode in Ni(TFSA)₂/BMPTFSA without and with ACN at 25 °C. Scan rate: 100 mV s⁻¹.

species. However, the cathodic peak potential shifted to the more negative side with an increase in the concentration of ACN among the ionic liquids containing ACN. When the concentration ratio of ACN to Ni²⁺ is less than 6, there may exist some mixed ligand complexes like [Ni(TFSA)_x(ACN)_{6-2x}]^{2-x-}, as suggested by the UV-vis spectroscopy (Fig. 1). Since the thermodynamic stability of [Ni(ACN)₆]²⁺ is expected to be higher than those of the mixed ligand complexes, the reduction potential was considered changed with the concentration of ACN [29].

The positive shift of the cathodic current peak in the cyclic voltammogram upon transformation from [Ni(TFSA)₃]⁻ to [Ni(ACN)₆]²⁺ suggests a decrease in the overpotential for reduction of Ni(II). Since the donor property of ACN is higher than TFSA⁻, the thermodynamic stability of [Ni(ACN)₆]²⁺ is considered higher than that of [Ni(TFSA)₃]⁻. Thus, the overpotential for reduction of [Ni(ACN)₆]²⁺ should be larger than that of [Ni(TFSA)₃]⁻. This inconsistency may be explained by the unique double layer structure in the ionic liquid. The ionic liquid does not contain any neutral molecule. Thus, the electrode surface is always in contact with the ions of ionic liquid. When the electrode is polarized negatively, the electrode surface will be charged negatively. Then, the population of positively charged species at the electrode-liquid interface must increase in order to compensate the negative charge on the electrode. In the absence of ACN, negatively charged [Ni(TFSA)₃]⁻ can not participate in the compensation at the interface. Thus, the electrode surface is covered dominantly with bulky BMP⁺. Therefore, the charge transfer between the electrode and [Ni(TFSA)₃]⁻ is expected to occur across the BMP⁺ layer (~0.7 nm thick). In addition, adsorption of nickel atoms may be hindered by adsorption of BMP⁺ on the electrode surface. Thus, the overpotential for reduction of [Ni(TFSA)₃]⁻ is expected to become very large. On the other hand, in case of addition of ACN, positively charged [Ni(ACN)₆]²⁺ can participate in the compensation at the interface, so that [Ni(ACN)₆]²⁺ is considered accessible to the electrode surface. Since this situation is very similar to that in conventional electrolytes, the overpotential for reduction of [Ni(ACN)₆]²⁺ is expected to be smaller than that of [Ni(TFSA)₃]⁻. The similar effect has been already found in electrodeposition of Co from BMPTFSA with addition of acetone [8].

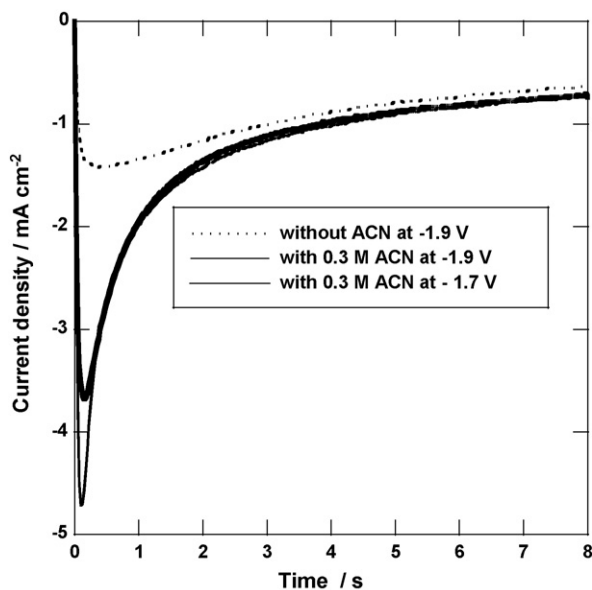


Fig. 5. Chronoamperograms of a Pt electrode in 0.05 M Ni(TFSA)₂/BMPTFSA without and with 0.3 M ACN at 25 °C.

3.3. Chronoamperogram

Fig. 5 shows the chronoamperograms of a Pt electrode in 0.05 M Ni(TFSA)₂/BMPTFSA without and with 0.3 M ACN. In the presence of 0.3 M ACN, sharp current peaks were observed after the charging of the electric double layer in the electrolyte and the current densities converged with the time, indicating the electrodeposition of Ni was controlled by the diffusion process, as observed in the ionic liquid without ACN [22]. The increase in the peak current density with ACN may suggest the increase in the number of nuclei formed on the substrate probably due to the adsorption of the positively charged species, [Ni(ACN)₆]²⁺.

The dependence of the viscosities of 0.05 M Ni(TFSA)₂/BMPTFSA without and with 0.3 M ACN on temperature (not shown) indicates that the viscosities of both ionic liquids decreased with elevating temperature according to the Andrade's formula ($\eta = A \exp(E_a/RT)$, A: constant). The activation energy for 0.05 M Ni(TFSA)₂/BMPTFSA with ACN for viscosities was 27.7 kJ mol⁻¹, which was slightly smaller than that without ACN (28.7 kJ mol⁻¹). There was little difference in the viscosity and its activation energy probably because no free ACN molecule existed in the ionic liquid with ACN.

According to the Cottrell's equation for semi-infinite one-dimensional diffusion [30], the diffusion coefficients of 0.05 M Ni(TFSA)₂/BMPTFSA without and with 0.3 M ACN at 25 °C were estimated to be 1.0×10^{-7} and 1.3×10^{-7} cm² s⁻¹, respectively. Based on the Stokes–Einstein relation, the diffusion of a charged species in a diluted solution is mostly determined by the size of the diffusing species and the viscosity of the solution. Since the viscosity of these two kinds of electrolytes has little difference (as described above), the difference in the diffusion coefficients between [Ni(ACN)₆]²⁺ and [Ni(TFSA)₃]⁻ is considered ascribed to that in the sizes of these complexes. The molar volumes of ACN and TFSA⁻ are estimated to be 53 and 159 cm³ mol⁻¹, respectively [31]. The total volume of coordinating ligands per mole in [Ni(TFSA)₃]⁻ is 477 cm³ mol⁻¹ while that of [Ni(ACN)₆]²⁺ is 318 cm³ mol⁻¹. Since the size of [Ni(ACN)₆]²⁺ is smaller than that of [Ni(TFSA)₃]⁻, the diffusion of [Ni(ACN)₆]²⁺ is expected to be faster than that of [Ni(TFSA)₃]⁻.

From the chronoamperometric results, the relationship between the non-dimensional parameters, $(j/j_m)^2$ and t/t_m , where j_m is the peak current density, t is the time and t_m is the time at j_m , is shown in Fig. 6. Compared to the theoretical model reported

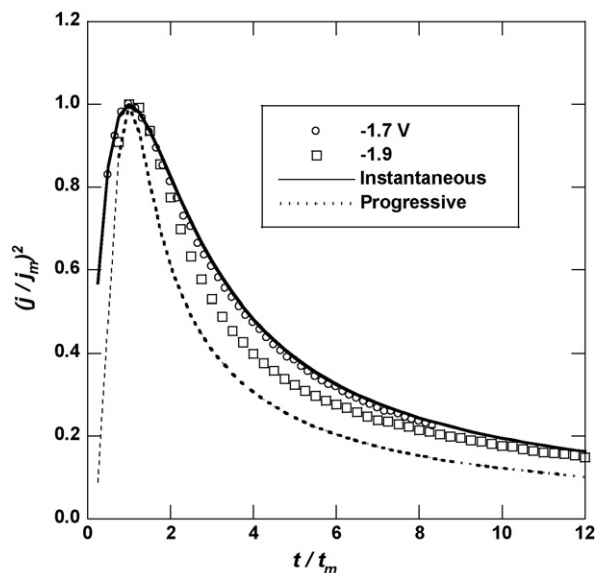


Fig. 6. Non-dimensional plots of $(j/j_m)^2$ vs. t/t_m from 0.05 M Ni(TFSA)₂/BMPTFSA with 0.3 M ACN at 25 °C.

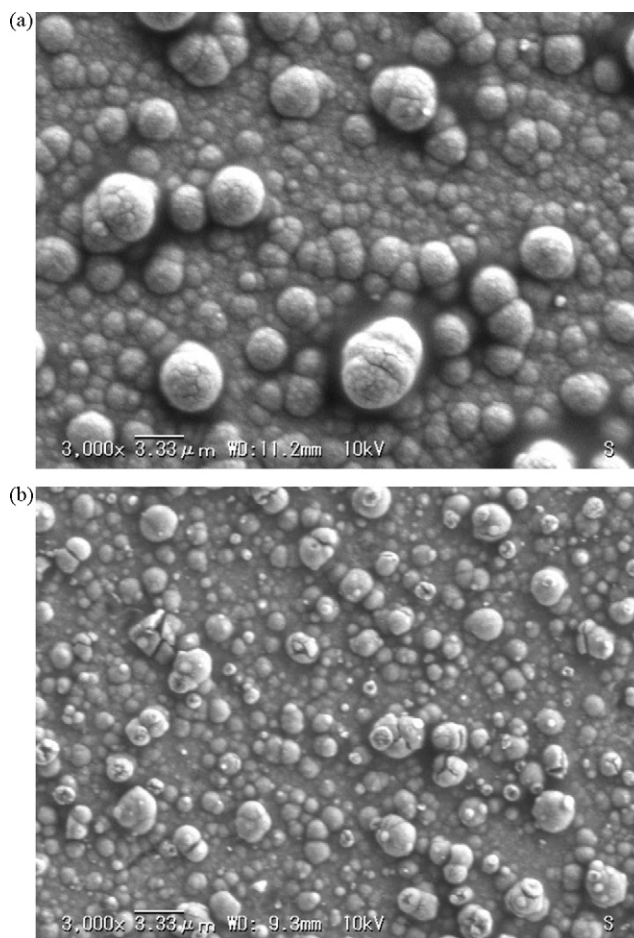


Fig. 7. SEM images of the deposits obtained on a Cu substrate in 0.05 M Ni(TFSA)₂/BMPTFSA (a) without and (b) with 0.3 M ACN at 50 °C. Current density: -0.05 mA cm⁻². Charge density: 3.6 C cm⁻².

by the Shaifker's nucleation and growth model [32], the initial stage of Ni deposition on a Pt electrode in the electrolyte with ACN can be explained better by instantaneous nucleation rather than progressive one. Thus, the nucleation mechanism was not affected by the change in the coordination environment of Ni^{2+} from $[\text{Ni}(\text{TFSA})_3]^-$ to $[\text{Ni}(\text{ACN})_6]^{2+}$ [22].

3.4. Electrodeposition of Ni

Electrodeposition of Ni on a copper substrate in 0.05 M $\text{Ni}(\text{TFSA})_2/\text{BMPTFSA}$ without and with 0.3 M ACN were performed by galvanostatic electrolysis with a current density of -0.05 mA cm^{-2} at 50°C . Fine-grained and smoother deposit was obtained in the presence of ACN, as shown in Fig. 7, probably related to an increase in the number of nuclei by formation of $[\text{Ni}(\text{ACN})_6]^{2+}$, as described above. The change in the morphology of electrode deposits is also considered related to the adsorption of $[\text{Ni}(\text{ACN})_6]^{2+}$ on the electrode. As described above, in the presence of ACN, $[\text{Ni}(\text{ACN})_6]^{2+}$ can access to the negatively charged electrode surface in addition to BMP^+ . If BMP^+ is assumed as an inhibitor for crystal growth, a decrease in the population of BMP^+ at the electrode surface is expected to promote crystal growth to give fine and granular deposits. In the absence of ACN, coarse and less adherent deposits are obtained probably because the active sites on the electrode surface are mainly dominated by BMP^+ .

4. Conclusions

The coordination environment of Ni(II) changed from $[\text{Ni}(\text{TFSA})_3]^-$ to $[\text{Ni}(\text{ACN})_6]^{2+}$ with addition of ACN in $\text{Ni}(\text{TFSA})_2/\text{BMPTFSA}$ due to the donor property of ACN being stronger than TFSA^- . This positively charged complexes made the reduction potential of Ni(II)/Ni shift to the more positive side and the diffusion coefficient of Ni(II) species become larger. The nucleation/growth mechanism of Ni(II)/Ni was not affected by addition of ACN into the ionic liquid. Fine-grained and smoother deposit was obtained by galvanostatic cathodic reduction in $\text{Ni}(\text{TFSA})_2/\text{BMPTFSA}$ with ACN. This result indicates that the additive is also important for controlling the electrode reactions and the morphology of the deposits in the ionic liquids, as known in the aqueous solutions. However, it is necessary to elucidate the detailed mechanism of the effects of these additives on the electrodeposition of metals in the ionic liquids.

Acknowledgment

The authors gratefully acknowledge the financial support of the Japanese Government (Monbukagakusho) Scholarship.

References

- [1] D. Landolt, *J. Electroanal. Chem.* 149 (2002) S9.
- [2] R.O. Kova, A. Turonova, D. Kladekova, M. Galova, R.M. Smith, *J. Appl. Electrochem.* 36 (2006) 957.
- [3] D. Golodnitsky, Y. Rosenberg, A. Ulus, *Electrochim. Acta* 47 (2002) 2707.
- [4] A. Ciszewski, S. Posluszny, G. Milczarek, M. Baraniak, *Surf. Coat. Technol.* 183 (2004) 127.
- [5] K.M. Yin, *J. Electrochem. Soc.* 144 (1997) 1560.
- [6] A.C. Mishra, A.K. Thakur, V. Srinivas, *J. Mater. Sci.* 44 (2009) 3520.
- [7] K.R. Marikkannu, G.P. Kalaigan, T. Vasudevan, *J. Alloys Compd.* 438 (2007) 332.
- [8] Y. Katayama, R. Fukui, T. Miura, *J. Electrochem. Soc.* 154 (2007) D534.
- [9] E.B. Sauhestre, *Plating* (1958) 1119.
- [10] C.C. Roth, H. Leidheiser, *J. Electrochem. Soc.* 100 (1953) 553.
- [11] M. Troyon, L. Wang, *Appl. Surf. Sci.* 103 (1996) 517.
- [12] L. Oniciu, L. Muresan, *J. Appl. Electrochem.* 21 (1991) 565.
- [13] T. Mimani, S.M. Mayanna, *J. Appl. Electrochem.* 23 (1993) 339.
- [14] N. Kaneko, N. Shinohara, Y. Itoh, H. Nezu, *Bunseki Kagaku* 40 (1991) 655.
- [15] Y. Nakamura, N. Kaneko, M. Watanabe, H. Nezu, *J. Appl. Electrochem.* 24 (1994) 227.
- [16] G.T. Rogers, M.J. Ware, *J. Electrochem. Soc.* 107 (1960) 677.
- [17] A. Bhandari, S.J. Hearne, B.W. Sheldon, S.K. Soni, *J. Electrochem. Soc.* 156 (2009) D279.
- [18] T.A. Costavaras, M. Froment, A.H. Goff, *J. Electrochem. Soc.* 120 (1973) 867.
- [19] A.P. Abbott, K.E. Ttaib, K.S. Ryder, E.L. Smith, *Trans. Inst. Met. Finish.* 86 (2008) 234.
- [20] P.X. Yang, M.Z. An, C.N. Su, F.P. Wang, *Chin. J. Inorg. Chem.* 25 (2009) 112.
- [21] J. Ding, J. Wu, D. MacFarlane, W.E. Price, G. Wallace, *Electrochem. Commun.* 10 (2008) 217.
- [22] Y.-L. Zhu, Y. Kozuma, Y. Katayama, T. Miura, *Electrochim. Acta* 54 (2009) 7502.
- [23] K. Fujii, T. Nonaka, Y. Akimoto, Y. Umabayashi, S. Ishiguro, *Anal. Sci.* 24 (2008) 1377.
- [24] M. Yamagata, Y. Katayama, T. Miura, *J. Electrochem. Soc.* 153 (2006) E5.
- [25] B.N. Figgis, *Introduction to Ligand Fields*, John Wiley and Sons, New York, London, 1966 (Chapter 9).
- [26] J.J. Baniewicz, J.A. Maguire, M.E. Munnell, M.L. Moore, *Thermochim. Acta* 12 (1975) 377.
- [27] M. Herstedt, M. Smirnov, P. Johansson, M. Chami, J. Grondin, L. Servant, J.C. Lassagues, *J. Raman Spectrosc.* 36 (2005) 762.
- [28] P. Johansson, S.P. Gejji, J. Tegenfeldt, J. Lindgren, *Electrochim. Acta* 43 (1998) 1375.
- [29] T.C. Franklin, *Surf. Coat. Technol.* 30 (1987) 415.
- [30] A.J. Bard, L.R. Faulkner, *Electrochemical Methods, Fundamentals and Applications*, 2nd ed., John Wiley and Sons, Inc., New York, 2001.
- [31] J. Jacquemin, P. Husson, V. Mayer, I. Cibulka, *J. Chem. Eng. Data* 52 (2007) 2204.
- [32] B. Scharifker, G. Hills, *Electrochim. Acta* 28 (1983) 879.